Chapter 2

Theory of Dielectric Relaxation in Solids

2.1 Introduction and Motivation: Technological importance of dielectrics in modern industry

Electrical insulators, the materials preventing the flow of current where it is not desired, have been used in the context of electrical engineering since the earliest days of the science and technology of electrical phenomena about a century and a half ago. The best modern insulating materials, which are often working under the most extreme external stresses, combine the ability to withstand elevated temperatures with other essential properties such as high breakdown strength, chemical inertness, long life, and low cost.

Although the first capacitor (or *condensor*) was constructed by Cunaeus and Musschenbroek as far back as 1745 [162] (it became very popular for a variety of experimental purposes under the name of Leyden jar), relatively little attention had been paid to the properties of insulating materials until 1837, when Faraday [163] published the first numerical measurements on these materials, which he called *dielectrics.* [164]

Faraday found that the capacity of a condensor was dependent on the nature of the material separating the conducting surfaces. This discovery encouraged further empirical studies of insulating materials aiming, among other things, at maximizing the amount of charge that can be stored by a capacitor.

Throughout most of the 19th century, scientists searching for insulating materials for specific applications have become increasingly concerned with the detailed physical mechanisms governing the behavior of these materials. By contrast with the insulation aspect, dielectric phenomena are both more general and more fundamental, as they are concerned more intimately with the microscopic mechanisms of dielectric polarization and include, especially, the transient behavior under time-varying electric fields.

The works by Mossotti [165, 166] and Clausius [167] marked the beginning of the systematic investigation of the dielectric properties, as they attempted to correlate the *specific inductive capacity,* a macroscopic characteristic of insulators introduced by Faraday [163] and now generally known as the *dielectric constant*, with the microscopic structure of the materials. Following Faraday in considering the dielectric to be composed of conducting spheres in a non-conducting medium, Clausius and Mossotti succeeded in deriving a relation between the dielectric constant ε and the volume fraction occupied by the conducting particles in the dielectric (see Section 2.2.3).

In the beginning of this century, Debye [168] realized that some molecules had permanent electric dipole moments associated with them, and that it is this molecular dipole moment that gives rise to the macroscopic dielectric properties of the materials.[1] Debye succeeded in extending the Clausius-Mossotti theory to take into account the permanent moments of the molecules, which allowed him and others to calculate molecular dipole moments from measurements of the dielectric constant. His theory, later extended by Onsager [170] and Kirkwood [171, 172] (see Section 2.2.3),

[1]The concept of molecules with a permanent dipole moment goes as far back as 1819, when Berzelius [169] described molecules to be composed of oppositely charged regions. In the nineteenth century this concept was also discussed by Clausius, von Helmholtz, and others (see Ref. [164] p. 3).

is in excellent agreement with experimental results for most polar liquids.

Debye's other major contribution to the theory of dielectrics was his application of the concept of molecular permanent dipole moments to explain the anomalous dispersion of the dielectric constant observed by Drude [173] and others. His theory (described in more detail in Section 2.3.3) linked this dispersion to the characteristic time (which he called *relaxation time*) needed for the permanent molecular dipoles to reorient (*relax*) following the changes in the externally applied electric field. For an alternating field, Debye deduced that the time lag between the average orientation of the moments and the field becomes noticeable when the frequency of the field is within the same order of magnitude as the reciprocal relaxation time. This way, the molecular relaxation process leads to the macroscopic phenomena of *dielectric relaxation*, *i.e.* the anomalous dispersion of the dielectric constant and the accompanying absorption of electromagnetic energy.

While in polar liquids, where the dipoles are relatively far away from each other, Debye's approach of treating a dielectric material as a collection of independent dipoles floating in a viscous non-polar liquid gives excellent agreement with experiment, the dielectric behavior of solids deviates considerably from what is predicted by Debye's theory. To correct this, several modifications and extensions of Debye's theory of dielectric relaxation have been proposed, each generally falling into one of the two following groups.

The first approach, pioneered by Cole [174], Davidson [175], and Williams [176], interprets the non-Debye relaxation behavior of the materials in terms of a superposition of exponentially relaxing processes, which then leads to a distribution of relaxation times. The second one proposes that the relaxation behavior at the molecular level is intrinsically non-Debye-like due to the cooperative molecular motions (the Jonscher's "many-body interactions" approach [177]).

After more than seventy years of development, the theory of dielectric relaxation is still very much an active area of research (see Section 2.3 for an overview of basic current theories). Understanding the behavior of dielectrics in varying electric fields is of particular importance for modern-day electronics, with its demand for dielectric materials with narrowly defined properties tailored for a particular application. For instance, the scaling of metal-oxide-semiconductor (MOS) devices for ultralarge scale integration (ULSI) applications has been placing an ever increasing burden upon the performance of gate dielectrics. Durability has become an issue as the dielectric thickness is decreased, leading to a search for dielectrics with better properties than, *e.g.*, thermal silicon oxide (SiO_2) commonly used in silicon-based electronic applications. And a gallium arsenide (GaAs) metal-insulator-semiconductor field effect transistor (MISFET, the basic building block for today's digital electronics technology) is still largely unavailable due to the lack of a suitable dielectric material for the insulation layer.[2]

The need for better dielectrics with improved properties suitable for modern integrated manufacturing needs was one of the main motivations for studying ways to enhance the dielectric properties of C_{60} thin films. And since in silicon technology, the enhancement of SiO_2 by nitrogen incorporation has been shown to result in an increased dielectric constant and resistance to impurity diffusion, as well as much higher resistance to interface state generation under avalanche, high-field, and hot-carrier stress, and irradiation (see, *e.g.*, Yount *et al.* [179] and references therein), a similar path has been chosen for attempting to improve the dielectric properties of fullerene solid films.[3] Chapter 4 is devoted to the discussion of experimental details and possible technological implications of various ways to introduce intercalants into the interstitial spaces of solid C_{60}.

[2]For recent advances in the attempts to create a molecularly designed insulator for this purpose, see, *e.g.*, Jenkins *et al.* [178]

[3]The use of fullerene composite thin films as gate dielectrics is the most immediate application that we had in mind in embarking on this project. It should be noted, however, that low-dielectric-constant materials, such as most fullerites, may also find applications in electronic packaging [180], as well as elsewhere in microelectronics [181].

2.2 Dielectrics in Static Fields

2.2.1 Electric susceptibility and permittivity

It was Michael Faraday [163] who first noticed that when a capacitor of value C_0 under vacuum is filled with a dielectric material, its charge storage capacity (*capacitance*) increases to a value C. The ratio χ' of the increase of capacitance $\Delta C = C - C_0$ to its initial capacitance C_0

$$\chi' = \frac{C - C_0}{C_0} = \frac{\Delta C}{C_0} \tag{2.1}$$

is called the *electric susceptibility* of the dielectric. Often, instead of the susceptibility, use is made of the *electric permittivity* (or *dielectric constant*), which is defined as the ratio of the capacitance C of a capacitor filled with the dielectric to the value C_0 of the same capacitor under vacuum:[4]

$$\varepsilon' = \frac{C}{C_0} \tag{2.2}$$

It follows from Eqns. (2.1) and (2.2) that the relation between the electric susceptibility and electric permittivity of a dielectric is

$$\chi' = \varepsilon' - 1 \tag{2.3}$$

Thus defined, the electric susceptibility and permittivity are non-dimensional real quantities.

2.2.2 Mechanisms of electric polarization

At the atomic level, all matter consists ultimately of positively and negatively charged particles whose charges balance each other macroscopically in the absence of an ex-

[4]Strictly speaking, the SI system defines the dielectric constant ε of a material as a product of its *relative dielectric constant* ε_r and the permittivity of free space ε_0: $\varepsilon = \varepsilon_r \varepsilon_0$. Our electric permittivity (dielectric constant) ε' is what SI calls the *relative* dielectric constant ε_r.

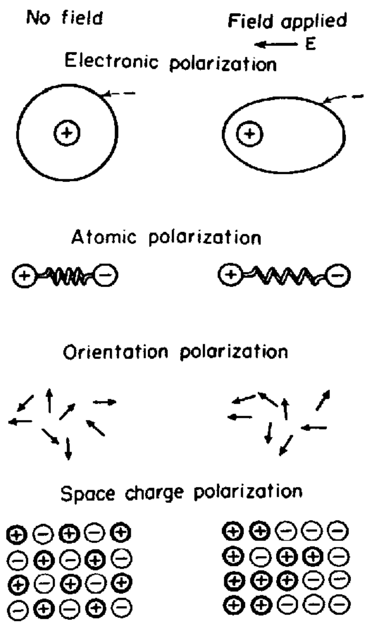

Figure 2-1: Mechanisms of polarization (after von Hippel [183]).

ternal electric field, giving rise to the overall charge neutrality of the material.[5] Once the electric field is applied, the balance of charges is perturbed by the following four basic polarization mechanisms (see Fig. 2-1).

Electronic polarization arises from the displacement of the electrons with respect to the atomic nuclei in the applied electric field. Electronic polarization is thus an *induced* polarization effect.

Atomic polarization is observed when different atoms that comprise a molecule share their electrons asymmetrically and cause the electron cloud to be shifted toward the stronger binding atoms. As a result, the atoms acquire charges of opposite polarity, and an external field acting on these net charges will tend to change the equilibrium positions of the atoms themselves creating this second

[5]In some materials, called *ferroelectrics* or *electrets*, the finite polarization is present even in the absence of the external electric field. [182] However, this effect of *permanent polarization* is beyond the scope of this work.

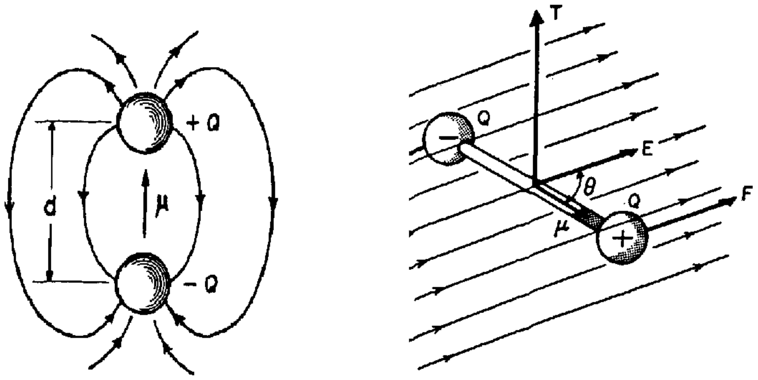

Figure 2-2: (a) Electric dipole of the moment $\vec{\mu} = Q\vec{d}$. (b) Torque $\vec{T} = \vec{\mu} \times \vec{E}$ acting on an electric dipole. (After von Hippel [183].)

type of *induced* polarization.

Orientational polarization, like the atomic polarization, is caused by the asymmetric charge distribution between the unlike components of a molecule. However, unlike the induced types of polarization, orientational (or *dipole*) polarization is created by *permanent* dipole moments, and exists also in the absence of an external field. Such moments experience a torque in an applied field (Fig. 2-2) that tends to orient them in the field direction.

Space-charge polarization is important in dielectric materials which contain charge carriers that can migrate for some distance through the bulk of the material (via, *e.g.*, diffusion, fast ionic conduction, or intercalation), thus creating a macroscopic field distortion. Such a distortion appears to an outside observer as an increase in the capacitance of the sample and may be indistinguishable from a real rise of the dielectric permittivity. Space-charge (or *interfacial*) polarization is the only type of electrical polarization that is accompanied by a macroscopic charge transport (and in the case when the migrating charge carriers are ions, a macroscopic mass transport as well).

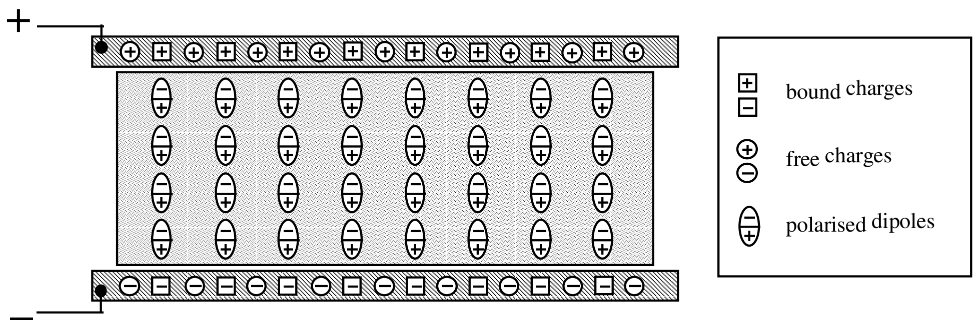

Figure 2-3: "Dipole chains" forming under the influence of an applied electric field bind countercharges with their free ends to the metal plates of the capacitor.

The total polarizability α of a dielectric material is a sum of these four contributions (see section 2.2.3 below). How these effects actually shape up the response characteristics of dielectrics will be discussed in section 2.3.

2.2.3 Static polarization

Suppose now that a dielectric material is inserted into an electric field E formed by the parallel plates of a capacitor. The charge storage capacity will be increased by neutralizing charges at the electrode surfaces which otherwise would contribute to the external field. This phenomenon of *dielectric polarization* can be visualized as the action of dipole chains which form under the influence of the applied field and bind countercharges with their free ends to the metal plates of the capacitor (see Fig. 2-3).

Generally, the polarization $\vec{P}$ of a dielectric material in a static electric field $\vec{E}$ depends on the electric field strength:

$$\vec{P} = \chi' \varepsilon_0 \vec{E} + o(\vec{E}^2), \tag{2.4}$$

where the dielectric susceptibility χ' is the proportionality factor, and $\varepsilon_0 = 8.854 \times 10^{-12}$ F/m is the electric permittivity of the vacuum. Retaining only the linear term

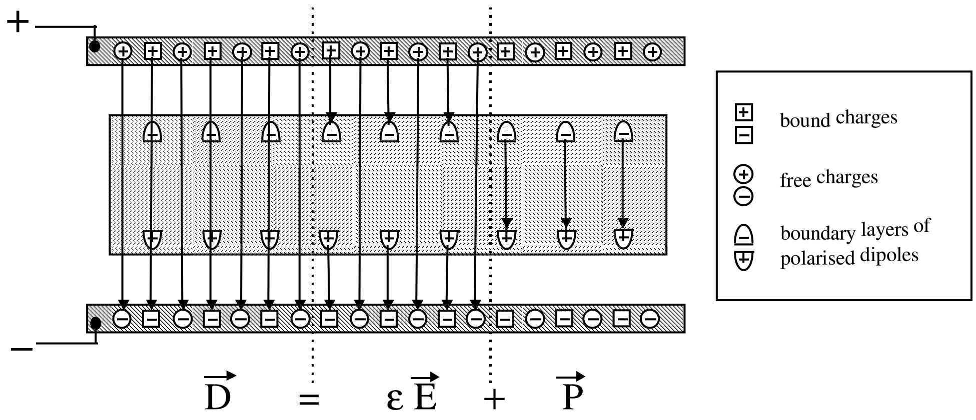

Figure 2-4: Dielectric in the electric field of a capacitor, showing field lines associated with $\vec{D}$ (free charge), $\varepsilon_0\vec{E}$ (all charges), and $\vec{P}$ (polarization charge).

in Eqn. (2.4) is sufficient for most isotropic dielectrics[6] provided that the strength of the applied field $\vec{E}$ is not very high. Keeping this in mind, the physical meaning of the electric susceptibility emerges:

$$\chi' = \frac{\vec{P}}{\varepsilon_0\vec{E}} = \frac{\text{bound charge density}}{\text{free charge density}}. \tag{2.5}$$

While the polarization vector $\vec{P}$ describes the polarization charge of the dielectric material, the electric displacement vector $\vec{D}$ (sometimes also called the *electric flux density*) is associated with the free charges collected on the plates of the capacitor. Using equations (2.3) and (2.4), we can therefore write for a linear dielectric medium

$$\vec{D} = \varepsilon_0\vec{E} + \vec{P} = (1+\chi')\varepsilon_0\vec{E} = \varepsilon'\varepsilon_0\vec{E}. \tag{2.6}$$

This relationship among the three vectors is illustrated by the Fig. 2-4.

A dielectric is described by a vector of dielectric polarization, and for that reason the electric susceptibility χ rather than the more usual electric permittivity ε is

[6]For non-isotopic dielectrics, the scalar susceptibility must be replaced by a tensor. Also, for ferroelectrics, Eqn. (2.4) is not true in general.

appropriate for describing the dielectric properties of a substance.[7] [177, 184] On the other hand, for an engineer who is interested in the phenomena taking place in a capacitor and its behavior in an electric field, the dielectric constant ε will have more relevance.

Static Polarizability

While the electric susceptibility and permittivity are the macroscopic characteristics of electric polarization, polarizability is its microscopic measure. As was mentioned in section 2.2.2 above, the total polarizability α of a dielectric material is a sum of the contributions from four polarization mechanisms:

$$\alpha = \alpha_e + \alpha_a + \alpha_o + \alpha_s \tag{2.7}$$

where α_e, α_a, α_o, and α_s are electronic, atomic (ionic), orientational (dipole), and space-charge (interfacial) polarizabilities, respectively. In the static and low-frequency fields that we shall be considering, the electronic polarizability α_e cannot be separated from the atomic polarizability α_a.[8] We shall therefore only be interested in the induced polarizability $\alpha_{ind} = \alpha_e + \alpha_a$ as a high-frequency "background" of the low-frequency dielectric behavior.

Non-Polar Dielectrics: Clausius-Mossotti and Lorentz-Lorenz equations

Let us first attempt to relate electric susceptibility and electric polarization for the case of non-polar dielectrics, in which the induced polarizability α_{ind} is the only type of polarizability present. To find the *internal* (or *local*) field $\vec{E}_A$ acting upon each

[7] For example, it will be shown later (Sec. 2.3.2) that the important parameter from the physical point of view is the phase shift between the polarization vector $\vec{P}$ and the electric field vector $\vec{E}$, and not between the electric displacement vector $\vec{D}$ and the electric vector $\vec{E}$.

[8] Purely electronic polarizability can be determined only in monatomic molecules where atomic polarization does not occur. Atomic polarization always occurs together with electronic polarization and, consequently, it can only be measured indirectly, usually by taking advantage of dispersion effects.[184, p. 20]

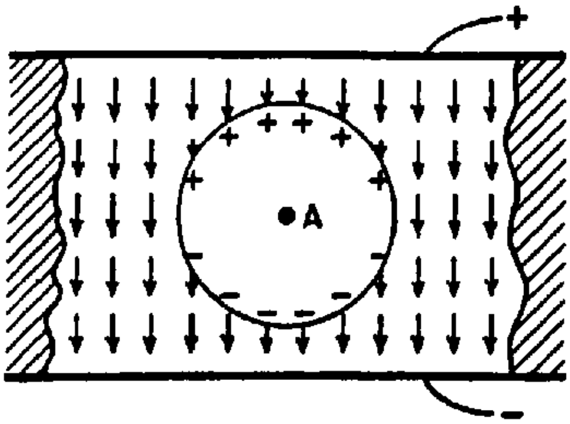

Figure 2-5: Model for calculation of Clausius-Mossotti internal field. (After von Hippel [183].)

molecule A of such a dielectric, we follow Mossotti [166] in constructing the following model (see Fig. 2-5).

Let the reference molecule A be surrounded by an imaginary sphere large enough to allow us to treat the dielectric outside it as a continuum. The total field $\vec{E}_A$ acting upon the molecule A can then be decomposed into the following three components:

$\vec{E}_1 = \vec{E}$ - the field due to the free charges at the capacitor plates, which, by definition, is equal to the applied electric field $\vec{E}$;

$\vec{E}_2 = \chi'\vec{E}/3$ - the field from the free ends of the dipole chains that line the cavity walls; and

$\vec{E}_3$ - the *near field* arising from the individual contributions of the molecules inside the sphere.

In the Clausius-Mossotti approximation, the near field $\vec{E}_3$ is set to zero, *i.e.* the additional individual field effects of the surrounding molecules on the particle A are presumed to cancel out. This roughly corresponds to the case of non-polar disordered weakly interacting matter, such as gases at moderate pressures. [164, p.172]

Macroscopically, the polarization $\vec{P}$ of a dielectric material was defined in Eqn. (2.4) as a function of the applied electric field:

$$\vec{P} = \chi'\varepsilon_0\vec{E}. \tag{2.8}$$

On the molecular level, on the other hand, polarization will depend on the locally acting electric field $\vec{E}_A$:

$$\vec{P} = N_m\alpha_{ind}\vec{E}_A \tag{2.9}$$

where N_m is the number of polarizable molecules per unit volume, and

$$\vec{E}_A = \vec{E}_1 + \vec{E}_2 + \vec{E}_3. \tag{2.10}$$

From the equations (2.3), (2.8), and (2.9) we get:

$$\frac{\chi'}{\chi' + 3} = \frac{\varepsilon' - 1}{\varepsilon' + 2} = \frac{N_m}{3\varepsilon_0}\alpha_{ind}. \tag{2.11}$$

This relation is generally called the *Clausius-Mossotti equation.* It interprets the static (low frequency) dielectric constant ε' of a medium (a macroscopic quantity), in terms of the polarizability α_{ind} of the contributing molecules (a microscopic parameter).

By using the *Maxwell relation* for a lossless (non-absorbing), non-magnetic medium

$$n^2 = \varepsilon', \tag{2.12}$$

where n is the *index of refraction* of the material, the equation (2.11) can be rewritten as

$$\frac{n^2 - 1}{n^2 + 2} = \frac{N_m}{3\varepsilon_0}\alpha_{ind}. \tag{2.13}$$

In this form, it is known as *Lorentz-Lorenz equation* [185, 186]. While it can be used to approximate the static dielectric constant ε' of non-polar non-magnetic materials from their optical properties (such as the index of refraction n), one should always keep in mind that such estimates will only be valid when the optical frequencies at which n is measured are low enough to incorporate the effects of the induced (electronic and atomic) polarization.

Polar Dielectrics: The Debye equation and the Mossotti catastrophe

In addition to the induced polarizability α_{ind} present in all dielectric materials, polar dielectrics possess orientational (dipole) polarizability α_o that exists even in the absence of an applied electric field. Because α_o has to do with reorientation of molecules, which are much heavier objects that either atoms or electrons responsible for the α_{ind}, α_o contributes to the total molecular polarizability α at much lower frequencies than α_{ind} does. For this reason, in the dielectric relaxation literature (which is mainly concerned with orientational polarizability), it is customary to designate the dielectric constant due to α_{ind} (or the *unrelaxed* dielectric constant) as ε_∞. In this notation, the Lorentz-Lorenz equation (2.13) becomes

$$\frac{\varepsilon_\infty - 1}{\varepsilon_\infty + 2} = \frac{N_m}{3\varepsilon_0}\alpha_{ind}. \tag{2.14}$$

To account for the orientational contribution to the dielectric constant, Debye [168] used classical Boltzmann statistics and the Langevin function $L(y) = \coth y - \frac{1}{y}$ from paramagnetism theory to estimate the temperature dependence of permanent-dipole orientation. Assuming that these dipoles do not interact with each other, Debye [168] derived the following formula for the orientational polarizability:

$$\alpha_o = \frac{\mu^2}{3kT}. \tag{2.15}$$

Using Clausius-Mossotti's "internal field" argument discussed above, this additional polarization contributes to the static dielectric constant according to the following formula (*cf.* Eqn. (2.11))

$$\frac{\varepsilon' - 1}{\varepsilon' + 2} = \frac{N_m}{3\varepsilon_0}\alpha_{ind} + \frac{N_d}{3\varepsilon_0}\alpha_o \tag{2.16}$$

where N_d is the number of dipolar molecules per unit volume (which may, of course, be the same as N_m).

Using Eqn. (2.13), we can now rewrite the Eqn. (2.16) in the following form, with the contribution of the orientational polarization of the permanent dipole set out separately:

$$\frac{\varepsilon' - 1}{\varepsilon' + 2} - \frac{\varepsilon_\infty - 1}{\varepsilon_\infty + 2} = \frac{N_d \mu^2}{9\varepsilon_0 kT}. \tag{2.17}$$

This result, due to Debye [187], has been used to successfully predict static dielectric constants of many polar gases and some polar liquids. However, when applied to the condensed state of matter, Debye's theory breaks down predicting infinite dielectric susceptibility (*Mossotti catastrophe*). The reason for this breakdown lies in the assumption that we made in the expression for the Clausius-Mossotti local field (2.10), setting the near field E_3 to zero. In condensed phases, permanent dipoles tend to lose their individual freedom of orientation through association and steric hindrance. Their interaction with their surroundings has to be taken into account, and the near field E_3 of Eqn. (2.10) cannot be neglected.

Polar Dielectrics: Onsager equation

To avoid the Mossotti catastrophe, Onsager [170] modified Debye's theory by introducing a different kind of cavity (see Fig. 2-6) with the following distinct properties:

- While the Clausius-Mossotti cavity is a mathematical fiction, the Onsager cavity is real, thus causing the electric field lines to be bent.

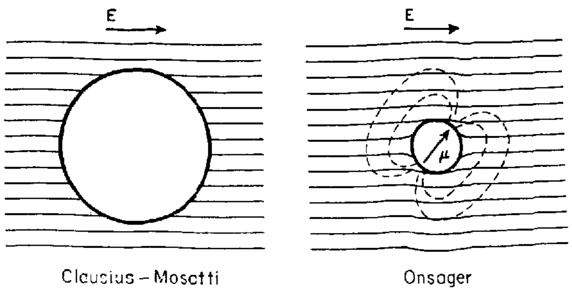

Figure 2-6: The Clausius-Mossotti and the Onsager cavities (after Van Vleck [188]).

- While the Clausius-Mossotti cavity contains a large number of molecules, the Onsager cavity encloses a single dipole molecule.
- While the center of the Clausius-Mossotti cavity is merely a mathematical point, the center of the Onsager cavity is marked by a point dipole which polarizes the surrounding medium. This polarization, acting back on the dipole in the cavity, creates the reaction field.

Based on these assumption, Onsager's theory arrives at the following expression linking the molecular dipole moment of the static dielectric constant [*cf.* Debye equation (2.17)]:

$$\frac{\varepsilon'-1}{\varepsilon'+2}-\frac{\varepsilon_\infty-1}{\varepsilon_\infty+2}=\frac{3\varepsilon'(\varepsilon_\infty+2)}{(2\varepsilon'+\varepsilon_\infty)(\varepsilon'+2)}\frac{N_d\mu^2}{9\varepsilon_0 kT}. \qquad (2.18)$$

In Fig. 2-7, equations (2.17) and (2.18) are solved[9]. for the dipole moment μ. We see that, for a given "induced" dielectric constant ($\varepsilon_\infty = 4$ in this case), the dipole moment calculated from the Debye model is significantly smaller than that calculated from the Onsager model, especially for large values of ε'. This indicates that the Clausius-Mossotti local field was considerably overestimated — the very fact that causes the Mossotti catastrophe.

[9]Mathcad Plus 6.0 for Microsoft Windows (MathSoft Inc., Cambridge, Mass.), a numerical and symbolic calculation software package, was used throughout this work.

Notation used in this worksheet:

Normalization factor: $A=9\varepsilon_0 kT/N$ $\quad A \equiv 1$

Dielectric constant (real part): ε'

"Unrelaxed" dielectric constant: ε_∞ (denoted as ε_{inf})

$$\mu_{Debye}(\varepsilon', \varepsilon_{inf}) := A \cdot \sqrt{\frac{3 \cdot (\varepsilon' - \varepsilon_{inf})}{(\varepsilon' + 2) \cdot (\varepsilon_{inf} + 2)}}$$

$$\mu_{Onsager}(\varepsilon', \varepsilon_{inf}) := A \cdot \sqrt{\frac{(2 \cdot \varepsilon' + \varepsilon_{inf}) \cdot (\varepsilon' - \varepsilon_{inf})}{\varepsilon' \cdot (\varepsilon_{inf} + 2)^2}}$$

$\varepsilon_{inf} := 4$ $\qquad \varepsilon' := \varepsilon_{inf}, \varepsilon_{inf} + 0.1 .. \varepsilon_{inf} + 35$

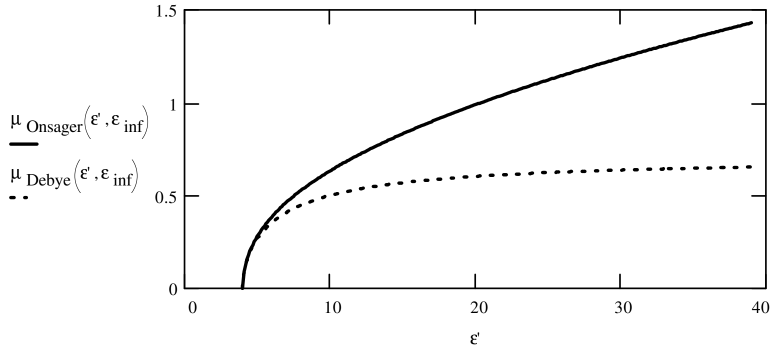

Figure 2-7: Mathcad worksheet illustrating the difference between Debye and Onsager results for the dipole moment μ. (Due to Mathcad's typesetting limitations, the dielectric constant due to induced polarization ε_∞ is shown as ε_{inf}.)

Space-Charge Polarization

Onsager's relation is quite well fulfilled for nonassociated polar liquids [189, p. 181], and can also be applied to weakly bound van der Waals solids, such as fullerites. In general, however, most solid dielectrics do not obey any of the local field expressions (Debye [187], Onsager [170], Kirkwood [171, 172], etc.) at sufficiently low frequencies due to the charge carriers present in these materials — mostly ions, but possibly also electrons. This renders any meaningful measurement of the low-frequency dielectric permittivity very difficult, making the comparison with local field theory rather doubtful.

2.3 Dielectrics in Time-Dependent Fields: Dielectric Relaxation

2.3.1 Maxwell's Equations

The most general formulation of the laws of electricity and magnetism is due to Maxwell [191] who in 1864 unified observations of Faraday, Gauss, and Ampere in the following four equations:

$$\nabla \times \vec{E}(\vec{r},t) = -\frac{\partial \vec{B}(\vec{r},t)}{\partial t} \qquad \text{(Faraday's law)} \tag{2.19}$$

$$\nabla \times \vec{H}(\vec{r},t) = \frac{\partial \vec{D}(\vec{r},t)}{\partial t} + \vec{J}(\vec{r},t) \qquad \text{(Ampere's law)} \tag{2.20}$$

$$\nabla \cdot \vec{D}(\vec{r},t) = \rho(\vec{r},t) \qquad \text{(Gauss's law)} \tag{2.21}$$

$$\nabla \cdot \vec{B}(\vec{r},t) = 0 \qquad \text{(Gauss's law)} \tag{2.22}$$

where the field variables[10] are defined as:

[10] Here the Maxwell's equations are written in the MKS (SI) "rationalized" system of units, which has been used exclusively throughout this work.

$\vec{E}$:	electric field	(volts/meter; V/m)
$\vec{H}$:	magnetic field	(amperes/meter; A/m)
$\vec{B}$:	magnetic flux density	(tesla; T)
$\vec{D}$:	electric displacement	
	(electric flux density)	(coulombs/meter^2; C/m^2)
$\vec{J}$:	electric current density	(amperes/meter^2; A/m^2)
ρ:	electric charge density	(coulombs/meter^3; C/m^3)

Maxwell's equations (2.19)–(2.22) describe the relation of these electric and magnetic fields to each other and to the position and motion of charged particles. Taking the divergence of Ampere's law (2.20) and making use of the Gauss's law (2.21), we obtain the *continuity equation* for the conservation of charge and current:

$$\frac{\partial \rho}{\partial t} + \nabla \cdot \vec{J} = 0. \tag{2.23}$$

This equation states that charge distributions which change in time give rise to currents, and has the important consequence that $\rho(\vec{r}, t)$ and $\vec{J}(\vec{r}, t)$ may not be specified independently.

In order to solve electrodynamic problems, a further set of relationships among the field quantities $\vec{D}$, $\vec{E}$, $\vec{B}$, and $\vec{H}$ must be established as there are more variables than equations contained within Maxwell's equations (2.19)–(2.22). These additional equations are known as *constitutive relations,* and they arise from physical consideration of the media in the problem to be solved. One such constitutive relation for *linear media* in the static case was arrived at in Eqn. (2.6) on page 83:

$$\vec{D}(\vec{r}, t) = \varepsilon_0 \varepsilon'(\vec{r}) \vec{E}(\vec{r}, t). \tag{2.24}$$

A corresponding relation for the magnetic flux density is

$$\vec{B}(\vec{r},t) = \mu_0 \mu'(\vec{r}) \vec{H}(\vec{r},t), \tag{2.25}$$

where $\mu_0 = 4\pi \times 10^{-7}$ H/m is the *permeability of free space*, and $\mu'(\vec{r})$ is the *relative permeability* of the material under study.

In the linear media described by constitutive relations (2.24) and (2.25), the Maxwell's equations (2.19)–(2.22) are linear, and therefore we can use the *superposition principle* to decompose any time-varying fields into a series of time-harmonics, for which solutions can be readily obtained. This procedure amounts to taking a Fourier transform of equations (2.19)–(2.22), which yields Maxwell equations in the frequency domain:

$$\begin{aligned} \nabla \times \vec{\mathbf{E}}(\vec{r}) &= -j\omega \vec{\mathbf{B}}(\vec{r}) && (2.26)\\ \nabla \times \vec{\mathbf{H}}(\vec{r}) &= j\omega \vec{\mathbf{D}}(\vec{r}) + \vec{\mathbf{J}}(\vec{r}) && (2.27)\\ \nabla \cdot \vec{\mathbf{D}}(\vec{r}) &= \boldsymbol{\rho}(\vec{r}) && (2.28)\\ \nabla \cdot \vec{\mathbf{B}}(\vec{r}) &= 0 && (2.29) \end{aligned}$$

The field variables are now expressed as complex phasors $\vec{\mathbf{E}}$, $\vec{\mathbf{H}}$, $\vec{\mathbf{D}}$, $\vec{\mathbf{B}}$, $\vec{\mathbf{J}}$, and $\boldsymbol{\rho}$, defined by $\vec{E}(\vec{r},t) = \mathrm{Re}\{\vec{\mathbf{E}}(\vec{r})e^{j\omega t}\}$, etc.

2.3.2 Complex Permittivity

Dielectric Response Function

In Section 2.2.3, the static polarizability of a linear medium was defined as $\vec{P} = \chi' \varepsilon_0 \vec{E}$, where χ' is the static dielectric susceptibility. In a time-varying electric field, the dielectric response of the medium is characterized by the *dielectric response function* $f(t)$ such that

$$P(t) = \varepsilon_0 (E_0 \delta t) f(t), \tag{2.30}$$

where $(E_0\delta t)$ is a delta-function excitation of strength E_0. For an arbitrary time-varying electric field $E(t)$, polarization $P(t)$ is then the result of the convolution integral

$$P(t) = f(t) \otimes \varepsilon_0 E(t) = \varepsilon_0 \int_0^\infty f(\tau)E(t-\tau)d\tau \tag{2.31}$$

Figure 2-8 shows a typical response of polarization $P(t)$ to a step-up excitation

$$\begin{aligned} E_{\mathrm{up}}(t) &= E_0 \quad \text{for} \quad t \geq 0 \\ &= 0 \quad \text{for} \quad t < 0 \end{aligned}$$

and a corresponding step-down excitation $E_{\mathrm{down}}(t)$. It is clear from the figure that, when the field E_0 is applied to the dielectric at time $t = 0$, the induced polarization P_{ind} is established very quickly — we can say instantaneously, compared with the time intervals of interest to us — but the remaining orientational part of the polarization takes time to reach its equilibrium (static) value P_{inf}.

Dielectric Susceptibility

While the dielectric response function $f(t)$ is an adequate and complete description of a dielectric, it is often more convenient to consider the dielectric response in the frequency domain. Equation 2.31 can generally be written

$$\vec{\mathbf{P}}(\omega) = \varepsilon_0 \boldsymbol{\chi}(\omega)\vec{\mathbf{E}}(\omega), \tag{2.32}$$

where $\vec{\mathbf{P}}(\omega)$ and $\vec{\mathbf{E}}(\omega)$ are the Fourier transforms of $\vec{P}(t)$ and $\vec{E}(t)$, respectively, while the frequency-dependent susceptibility $\boldsymbol{\chi}(\omega)$ is defined as the transform of the dielectric response function $f(t)$:

$$\boldsymbol{\chi}(\omega) = \chi'(\omega) - j\chi''(\omega) = \frac{1}{2\pi}\int_0^\infty f(t)e^{-j\omega t}dt. \tag{2.33}$$

We calculate the polarization $P_{up}(t)$ and $P_{down}(t)$ of a dielectric in response to the step excitations $E_{up}(t)$ and $E_{down}(t)$, respectively:

$$E_{up}(t) := \begin{cases} E_0 & \text{if } t \geq 0 \\ 0 & \text{otherwise} \end{cases} \qquad E_{down}(t) := \begin{cases} E_0 & \text{if } t < 0 \\ 0 & \text{otherwise} \end{cases}$$

As shown in the text, polarization is, in this case:

$$P_{up}(t) := P_{ind} + \varepsilon_0 \cdot E_0 \cdot \int_0^t f(\tau)\, d\tau \qquad P_{down}(t) := \left(P_{inf} - P_{ind}\right) - \varepsilon_0 \cdot E_0 \cdot \int_0^t f(\tau)\, d\tau$$

where P_{ind} is the "instantaneous" polarization due to induced polarizability, P_{inf} is the asymptotic (relaxed) polarization at infinitely long charging time, and $f(t)$ is the dielectric response function. The step-up and step-down polarization responses are plotted below for a typical dielectric response function

$$f(t) := \left(P_{inf} - P_{ind}\right) \cdot e^{-\left(\frac{t}{\tau_0}\right)}$$

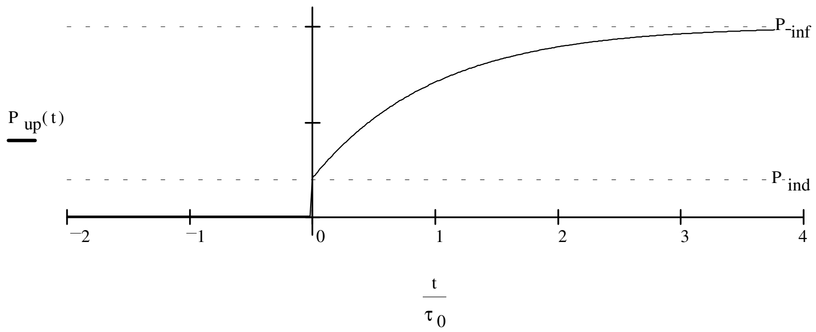

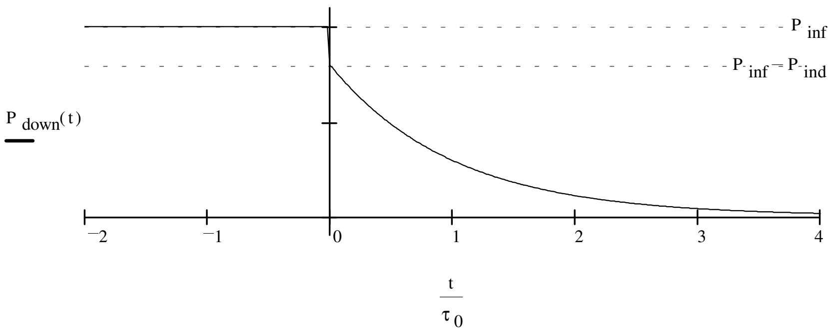

Figure 2-8: Mathcad worksheet showing the response of the polarization of a dielectric to the step-up and step-down excitations.

The susceptibility is a *complex* function of frequency, reflecting the fact that it contains information about both the amplitude and the phase angle of the components of the polarization. While the real part $\chi'(\omega)$ gives the amplitude of polarization in phase with the harmonic driving field, the imaginary part $\chi''(\omega)$ (also known as *dielectric loss*) gives the component in quadrature with the field.

Since, from the physical considerations, susceptibility $\chi(\omega)$ is a causal function, its real and imaginary parts can be expressed as Hilbert transforms of each other:

$$\chi'(\omega) = \frac{1}{\pi}\int_{\infty}^{\infty} \frac{\chi''(x)}{x-\omega}dx \tag{2.34}$$

$$\chi''(\omega) = -\frac{1}{\pi}\int_{\infty}^{\infty} \frac{\chi'(x)}{x-\omega}dx. \tag{2.35}$$

These integrals, known as *Kramers-Kronig relations*, are sometimes more conveniently written in the one-sided form:

$$\chi'(\omega) = \frac{2}{\pi}\int_{0}^{\infty} \frac{x\chi''(x)}{x^2-\omega^2}dx \tag{2.36}$$

$$\chi''(\omega) = -\frac{2\omega}{\pi}\int_{0}^{\infty} \frac{\chi'(x)}{x^2-\omega^2}dx. \tag{2.37}$$

One very immediate consequence of the Kramers-Kronig relations is their interpretation of the static susceptibility. Evaluation Eqn. 2.36 at $\omega = 0$ yields:

$$\chi'(0) = \frac{2}{\pi}\int_{0}^{\infty} \frac{\chi''(x)}{x}dx = \frac{2}{\pi}\int_{0}^{\infty} \chi''(x)d(\ln x). \tag{2.38}$$

This expression relates the polarization increment for a given polarization mechanism to the area of the loss curve plotted against the natural logarithm of the frequency. [177] This shows that a mechanism leading to a strong polarization must be associated with a correspondingly high loss.

Dielectric Permittivity

The frequency-domain response of a dielectric medium may also be written in terms of the *dielectric permittivity* $\varepsilon(\omega)$, which is defined by the constitutive relation (2.24) as

$$\vec{\mathbf{D}}(\omega) = \varepsilon_0 \varepsilon(\omega) \vec{\mathbf{E}}(\omega) = \varepsilon_0 \left[1 + \chi'(\omega) - j\chi''(\omega)\right] \vec{\mathbf{E}}(\omega). \tag{2.39}$$

The real part of $\varepsilon(\omega)$ consists of the contributions of free space and the real part of the susceptibility of the medium itself, while the imaginary component is entirely due to the medium. In the case where the medium has several polarization mechanisms coexisting and not significantly interacting among themselves, the permittivity can be expressed as the sum of the contributions of the individual mechanisms:

$$\varepsilon(\omega) = \varepsilon_0 \left[1 + \sum_{\alpha} \chi'_{\alpha}(\omega) - j \sum_{\alpha} \chi''_{\alpha}(\omega)\right] \equiv \varepsilon'(\omega) - j\varepsilon''(\omega) \tag{2.40}$$

where summation extends over all the separate polarization mechanisms labeled with the index α [177]. Figure 2-9 illustrates how the real part $\varepsilon'(\omega)$ of the permittivity is made up of contributions of all loss processes at frequencies higher than the frequency in question. The real part of the susceptibility $\chi'_{\alpha}(\omega)$ of every process adds to the sum of the contributions of all higher processes which define the "high frequency permittivity" $\varepsilon_{\infty\alpha}$ for that process.

Generally, the dielectric permittivity $\varepsilon'(\omega)$ of a material measures the polarization of the material per unit electric field. Interfacial, orientational, atomic, and electronic polarization mechanisms (see section 2.2.2) contribute to the total (static) dielectric constant $\varepsilon(0)$ at a frequency characteristic each mechanism. The time required for polarization to occur is directly related to the distance over which charge is being displaced, and the ease with which it can be displaced. (see Fig. 2-10). Interfacial polarization, which depends on the detailed electrode configuration, is generally not observed at frequencies above 1000 Hz [192]; orientational polarization typically takes place at frequencies below 1 MHz; atomic polarization arises with molecular vibrations

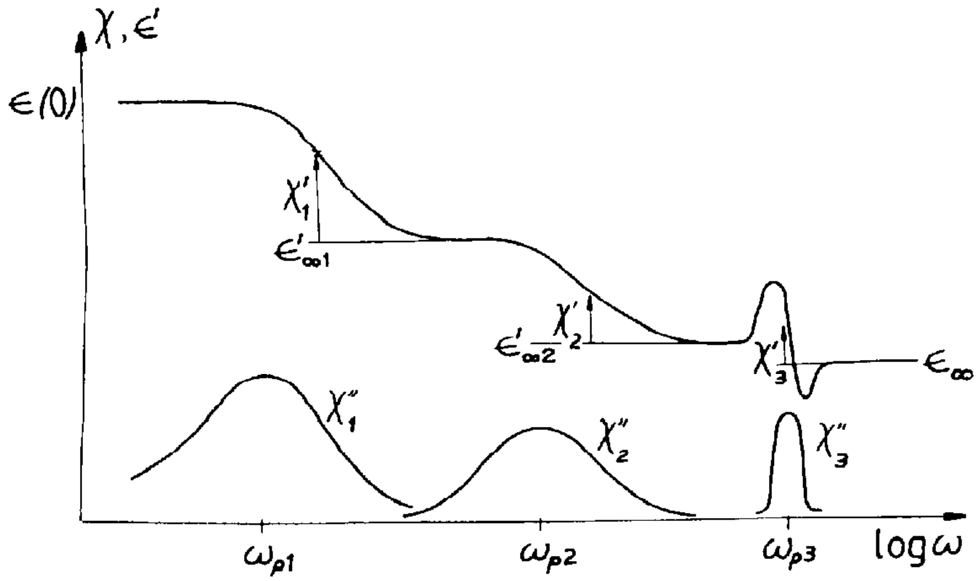

Figure 2-9: An illustration of the manner in which the static dielectric permittivity $\varepsilon(0)$ is made up of contributions of all loss processes. Three contributing processes are shown, denoted by the subscripts $\alpha = 1, 2, 3$ (the process associated with χ_3 being a resonance process). (after Jonscher [177]).

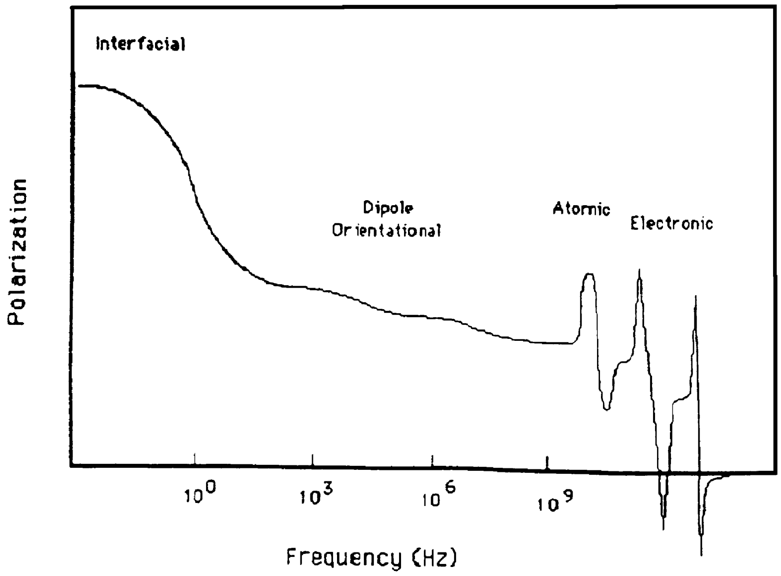

Figure 2-10: Dispersion of polarization in dielectric measurements is caused by four different polarization mechanisms (interfacial, dipole/orientational, atomic, and electronic) each contributing at its own characteristic frequency.

at frequencies around 10^9–10^{13} Hz, and electronic polarization shows up at optical frequencies (10^{14}–10^{16} Hz).

In our discussion of the dielectric relaxation, we shall constrain ourselves to the low frequency range of 10^{-3}–10^5 Hz, where orientational and interfacial polarization processes are the only contributors to $\varepsilon(0)$. The "unrelaxed," permittivity ε_∞ due to induced polarization will, therefore, be considered frequency-independent for the purposes of this study.

Effective Dielectric Constant

Since all actual dielectric media invariably possess a finite (although, possibly, very small) DC conductivity σ_0, this DC contribution will show up in any measurement of the dielectric response. Let us suppose that the dielectric medium under consideration is isotropic, and that, at $\omega = 0$, the *Ohm's law* (which is merely another experimentally verified constitutive relation) holds:

$$\vec{\mathbf{J}} = \sigma_0 \vec{\mathbf{E}}. \tag{2.41}$$

By applying Ohm's Law (2.41) and using Eqn. (2.39), the Ampere's Law (2.27) can be written

$$\begin{aligned} \nabla \times \vec{\mathbf{H}}(\omega) &= j\omega\varepsilon_0\varepsilon(\omega)\vec{\mathbf{E}}(\omega) + \sigma_0\vec{\mathbf{E}}(\omega) \\ &= j\omega\varepsilon_0\varepsilon_{\text{eff}}(\omega)\vec{\mathbf{E}}(\omega), \end{aligned} \tag{2.42}$$

where $\varepsilon_{\text{eff}}(\omega)$ was chosen such that

$$\varepsilon_{\text{eff}}(\omega) = \varepsilon(\omega) - j\frac{\sigma_0}{\omega\varepsilon_0}. \tag{2.43}$$

By substituting Eqn.(2.40) we get:

$$\varepsilon_{\text{eff}}(\omega) = \varepsilon'(\omega) - j\left(\varepsilon''(\omega) + \frac{\sigma_0}{\omega\varepsilon_0}\right). \tag{2.44}$$

Eqn. (2.44) demonstrates that DC conductivity shows up as increased loss in a dielectric measurememnt. Furthermore, even if σ_0 is relatively small (as is the case in the insulators), it may dominate $\varepsilon_{\text{eff}}(\omega)$ at sufficiently low frequencies. In order to extract the actual permittivity of the material $\varepsilon(\omega)$ from the measured permittivity $\varepsilon_{\text{eff}}(\omega)$, an independent measurement of σ_0 is required.

2.3.3 Microscopic Models of Dielectric Relaxation

The motion of dipoles in the electric field gives rise to frequency-dependent contributions to the permittivity $\varepsilon'(\omega)$ and the loss factor $\varepsilon''(\omega)$. Figure 2-11 illustrates in a highly schematic manner the alignment of molecular dipoles in an applied electric field. Because the dipoles are rigidly attached to relatively large molecules in a

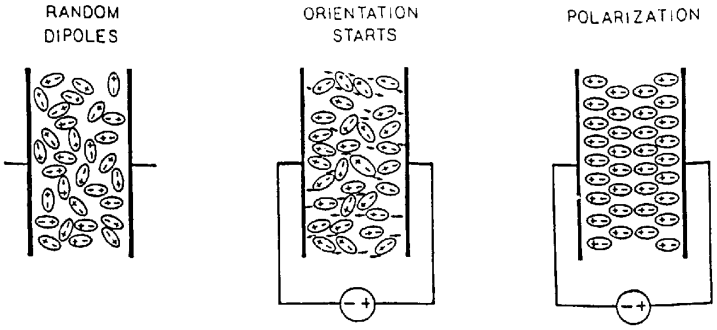

Figure 2-11: Idealized view of the polarization due to dipole orientation in the presence of an applied electric filed (after Day *et al.* [193]).

viscous medium, the orientation process can be characterized by a *dipole relaxation time* τ_d. Because of the hindering mechanism, there is energy loss associated with the orientation process.

The classical Debye theory: A single relaxation time

Debye [187] developed a model for the complex permittivity $\varepsilon(\omega)$ of a spherical polar molecule relaxing in a viscous medium, based on the assumption of a single relaxation time τ_d for all molecules:

$$\frac{\varepsilon(\omega) - \varepsilon_\infty}{\varepsilon(0) - \varepsilon_\infty} = \frac{1}{1 + j\omega\tau_d}, \tag{2.45}$$

where $\omega = 2\pi f$ is the angular frequency. The expression for the *normalized complex permittivity* $\frac{\varepsilon(\omega)-\varepsilon_\infty}{\varepsilon(0)-\varepsilon_\infty}$ is conventionally used to isolate the frequency dependence of complex permittivity for a particular polarization mechanism, where ε_∞ is used in the sense suggested by the Fig. 2-9. Separating Eqn. (2.45) into real and imaginary parts yields the relative permittivity $\varepsilon'(\omega)$ and loss factor $\varepsilon''(\omega)$, respectively:

$$\varepsilon'(\omega) = \varepsilon_\infty + \frac{\varepsilon(0) - \varepsilon_\infty}{1 + (\omega\tau_d)^2} \tag{2.46}$$

$$\varepsilon''(\omega) = \frac{(\varepsilon(0) - \varepsilon_\infty)\omega\tau_d}{1 + (\omega\tau_d)^2}. \tag{2.47}$$

Note that these equations assume that the material's DC conductivity $\sigma(0)$ is equal to zero. Ionic conductivity makes additional contribution to ε'', and can also lead to electrode polarization. These effects are discussed below in Sec. 2.3.4.

To explain the microscopic origins of the relaxation time τ_d, Debye developed a relationship between τ_d and the viscous friction η experienced by a spherical molecule of radius a:

$$\tau_d = \frac{4\pi a^3 \eta}{kT}. \tag{2.48}$$

The relaxation time is thus expected to be directly proportional to the microscopic viscosity experienced by the molecule. While this has been observed qualitatively [175], the quantitative calculations of the molecular size a from the relaxation time and viscosity measurements have not been very successful, because the macroscopic viscosity does not adequately describe the viscous friction experienced by the molecule [194].

The dependence of the permittivity and loss factor of the Debye model on the angular frequency ω is illustrated in Fig. 2-12. At frequencies much lower than $1/2\pi\tau_d$, when dipoles have sufficient time to orient along the applied field, the permittivity approaches the relaxed value $\varepsilon'(0)$ and the loss factor ε'' approaches zero. At high frequencies ($f \gg 1/2\pi\tau_d$), when dipoles are unable to orient, the permittivity approaches its unrelaxed value ε_∞ and the loss factor again approaches zero. At $f = 1/2\pi\tau_d$ the permittivity decreases from $\varepsilon'(0)$ to ε_∞ with increasing frequency, and the loss factor peaks out at $\varepsilon'' = \frac{1}{2}[\varepsilon'(0) - \varepsilon_\infty]$.

Deviations from the Debye behavior: A "distribution of relaxation times" approach

The width of the Debye relaxation at half maximum is only 1.4 decades. In real materials, however, the region of frequency dispersion extends over much larger frequency range than the Debye model predicts, because the dipolar hindering mechanisms are

Notation used in this worksheet: $\varepsilon_{inf} = \varepsilon_{\infty}$; $\varepsilon_0 = \varepsilon(0)$; $\omega = 2\cdot\pi\cdot f$

Permittivity $\varepsilon'(\omega)$ and loss $\varepsilon''(\omega)$ are defined as follows:

$$\varepsilon'(f) := \varepsilon_{inf} + \frac{\varepsilon_0 - \varepsilon_{inf}}{1 + \left(2\cdot\pi\cdot f\cdot\tau_d\right)^2} \qquad \varepsilon''(f) := \frac{\left(\varepsilon_0 - \varepsilon_{inf}\right)\cdot 2\cdot\pi\cdot f\cdot\tau_d}{1 + \left(2\cdot\pi\cdot f\cdot\tau_d\right)^2}$$

Permittivity and Loss are plotted below for τ_d=0.001sec and f=1Hz..30000Hz

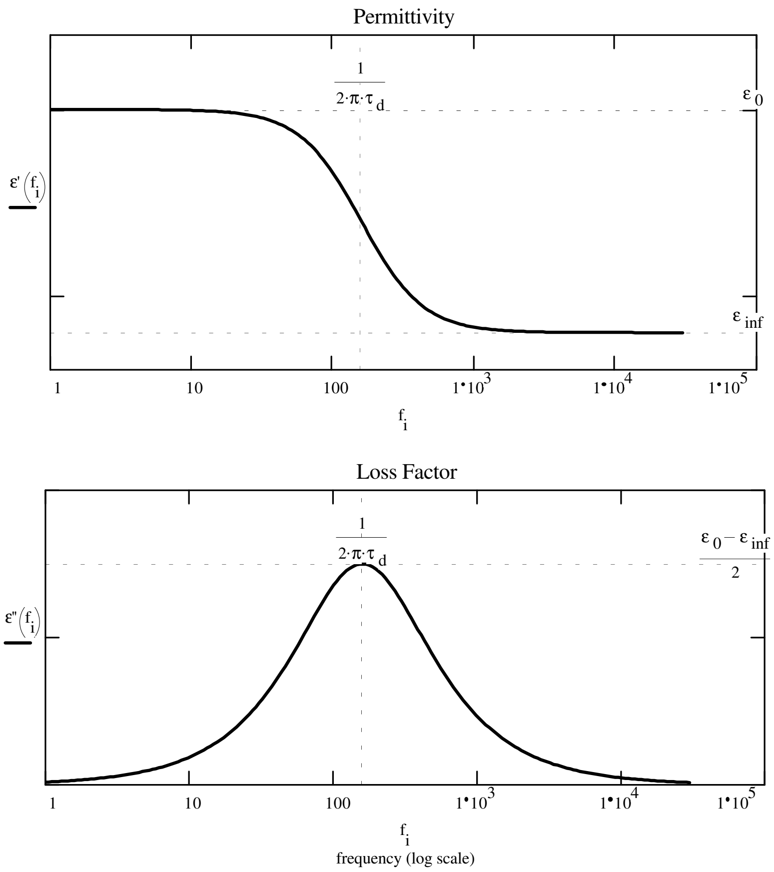

Figure 2-12: Mathcad worksheet showing the frequency dependence of the Debye single relaxation time model for dipole orientation.

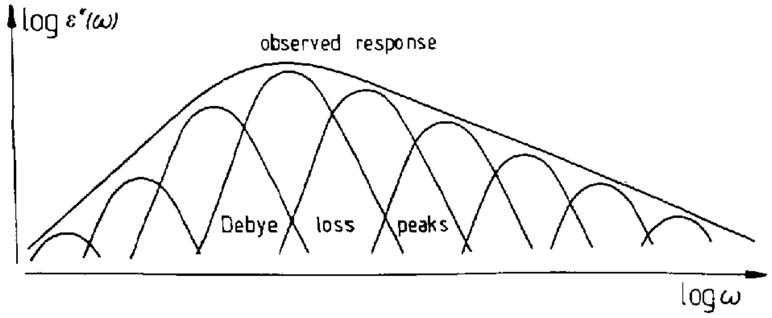

Figure 2-13: A schematic representation of the significance of the existence of a distribution of relaxation times in the application to the interpretation of a "non-Debye" loss peak in a dielectric material (after Jonscher [177]).

not characterized by a single τ_d but by a distribution of relaxation times $G(\tau)$. This broader dispersion characterized by $G(\tau)$ can be described in terms of the superposition of Debye-like relaxation processes as an integral (*cf.* Eqn. (2.45))

$$\frac{\varepsilon(\omega) - \varepsilon_\infty}{\varepsilon(0) - \varepsilon_\infty} = \int_{-\infty}^{\infty} \frac{G(\tau/\tau_d)}{1 + j\omega\tau_d} d\ln(\tau/\tau_d), \tag{2.49}$$

where a normalized form $G(\tau/\tau_d)$ was used for the distribution function. This operation may be represented graphically by the construction show in Fig. 2-13. It is evident that, within very wide limits, any sufficiently slowly varying function of frequency $\varepsilon(\omega)$ may be represented by the integral in Eqn. (2.49), so that virtually all forms of relaxation behavior can be "explained" by this means [177].

The concept of a distribution of relaxation times was first proposed by von Schweidler [195]. Later Wagner [196] suggested the use of a Gaussian distribution, but the quantitative evaluation of this and other proposals that followed was prohibitively cumbersome until Cole and Cole [174] developed a method to evaluate how well the permittivity and loss factor agreed with the Debye model. Cole and Cole found [174] that a plot of $\varepsilon''(\omega)$ from Eqn. (2.47) versus $\varepsilon'(\omega)$ from Eqn. (2.46), with $\omega\tau_d$ as a parameter, results in a semicircle (Fig. 2-14), and that for most materials, the locus

In the following Cole-Cole plot, $k = \omega \cdot \tau_d$ is used as the parameter.

In this notation, the permittivity and loss for the Debye model become:

$$\varepsilon'(k) := \varepsilon_{inf} + \frac{\varepsilon_0 - \varepsilon_{inf}}{1 + k^2} \qquad \varepsilon''(k) := \frac{(\varepsilon_0 - \varepsilon_{inf}) \cdot k}{1 + k^2}$$

The Cole-Cole plot for the Debye model is plotted below for $k := 0.01, 0.05 .. 100$

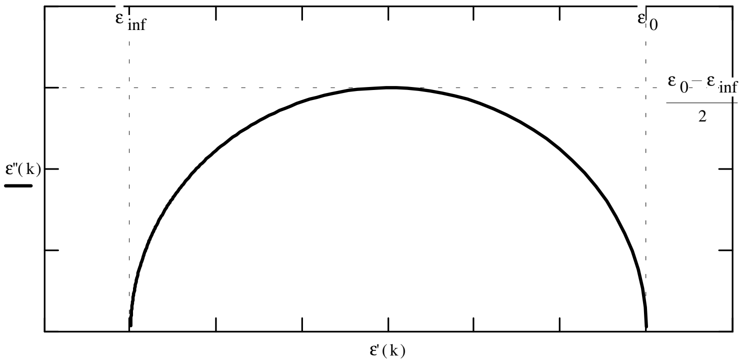

Figure 2-14: Mathcad worksheet showing a Cole-Cole plot of the Debye single relaxation time model for dipole orientation.

of experimental data fell *inside* this semicircle. Cole and Cole observed that the locus often formed the arc of a circle having a center depressed below the $\varepsilon'' = 0$ axis, and proposed that the data could be described empirically by a modified Debye equation,

$$\frac{\varepsilon(\omega) - \varepsilon_\infty}{\varepsilon(0) - \varepsilon_\infty} = \frac{1}{1 + (j\omega\tau_{\mathrm{CC}})^{\beta_{\mathrm{CC}}}}, \tag{2.50}$$

where the exponent β_{CC} is known as the distribution parameter that characterizes the breadth of the relaxation time distribution and ranges from 0 (infinitely broad distribution) to 1 (Debye's single relaxation time limit). This empirical function implicitly defines a functional form of the distribution of relaxation times,

$$G_{\mathrm{CC}}(\tau/\tau_{\mathrm{CC}}) = \frac{1}{2\pi} \frac{\sin[\pi(1 - \beta_{\mathrm{CC}})]}{\cosh[\beta_{\mathrm{CC}} \ln(\tau/\tau_{\mathrm{CC}})] - \cos[\pi(1 - \beta_{\mathrm{CC}})]}, \tag{2.51}$$

which is symmetrical and centered about the value τ_{CC} (see Fig. 2-17). The Cole-Cole relaxation equation (2.50) is compared to the Debye model for $\beta = 0.7$ and $\beta = 0.4$ on Fig. 2-16.

Another empirical function describing some experimental dielectric relaxations was proposed by Davidson and Cole [175]. This function expresses the complex dielectric constant as

$$\frac{\varepsilon(\omega) - \varepsilon_\infty}{\varepsilon(0) - \varepsilon_\infty} = \frac{1}{(1 + j\omega\tau_{\mathrm{CD}})^{\beta_{\mathrm{CD}}}}, \tag{2.52}$$

where τ_{CD} is the Davidson-Cole time constant, and the distribution parameter β_{CD} is similar to that of the Cole-Cole distribution (see Fig. 2-16). The corresponding distribution of the relaxation times

$$\begin{aligned} G_{\mathrm{CD}}(\tau/\tau_{\mathrm{CD}}) &= \frac{\sin \pi\beta_{\mathrm{CD}}}{\pi} \left(\frac{\tau}{\tau_{\mathrm{CD}} - \tau}\right)^{\beta_{\mathrm{CD}}}, \tau < \tau_{\mathrm{CD}} \\ &= 0, \tau > \tau_{\mathrm{CD}} \end{aligned} \tag{2.53}$$

is one-sided (see Fig. 2-17 and Table 2.3.3); there are no relaxation times below the value τ_{CD}. The maximum loss for this case occurs not at $\langle f \rangle = 1/2\pi\tau$ (as in the Debye and Cole-Cole distributions), but at

$$\langle f \rangle_{\mathrm{CD}} = \frac{1}{2\pi\tau_{\mathrm{CD}}} \tan\left(\frac{1}{\beta_{\mathrm{CD}} + 1}\frac{\pi}{2}\right) \tag{2.54}$$

While the physical significance of this relaxation time distribution is unclear, a relaxation function of this form has been derived using a defect diffusion model [197].

Perhaps, the most popular empirical relaxation function was proposed by Williams and Watts [176, 198]. Like the Davidson-Cole function, the Williams-Watts relaxation gives rise to a skewed Cole-Cole diagram, which fits well to a large number of relaxation data for polymers and glasses. The Williams-Watts function is derived by assuming that the time decay of the polarization is expressed by the stretched exponential function,

$$P_{\mathrm{WW}}(t) = e^{-\left(\frac{t}{\tau_{\mathrm{WW}}}\right)^{\beta_{\mathrm{WW}}}}, \tag{2.55}$$

where $\tau_{\rm ww}$ is the Williams-Watts time constant, and the distribution parameter[11] $\beta_{\rm ww}$ ranges from 0 to 1 (at $\beta_{\rm ww} = 1$ the expression reduces to the Debye single relaxation time case; see Table 2.3.3 for more informations). Fourier-transforming the stretched exponential decay function, Williams and Watts [198] derived the following expression for the complex dielectric constant (see Fig. 2-16):

$$\frac{\varepsilon(\omega)-\varepsilon_\infty}{\varepsilon(0)-\varepsilon_\infty} = \sum_{n=1}^{\infty} \frac{(-1)^{n-1}}{(\omega\tau_{\rm ww})^{n\beta_{\rm ww}}} \frac{\Gamma(n\beta_{\rm ww}+1)}{\Gamma(n+1)} \left[\cos\left(\beta_{\rm ww}\frac{n\pi}{2}\right) - j\sin\left(\beta_{\rm ww}\frac{n\pi}{2}\right)\right]. \quad (2.56)$$

The relaxation time distribution function for the Williams-Watts relaxation can also be solved in a closed form:

$$G_{\rm ww}(\tau/\tau_{\rm ww}) = -\frac{\tau_{\rm ww}}{\pi\tau}\sum_{n=1}^{\infty}\frac{(-1)^n}{n!}\sin(\pi\beta_{\rm ww}n)\Gamma(\beta_{\rm ww}n+1)\left(\frac{\tau}{\tau_{\rm ww}}\right)^{\beta_{\rm ww}n+1}. \quad (2.57)$$

It is instructive to plot the Williams-Watts distribution function $G_{\rm ww}(\tau/\tau_{\rm ww})$ for different values of $\beta_{\rm ww}$ (see Fig. 2-15). It is asymmetric about $\tau/\tau_{\rm ww} = 1$ when plotted *vs* $\log(\tau/\tau_{\rm ww})$, has a greater fraction of relaxation times above the value $\tau_{\rm ww}$, and exhibits a maximum with an amplitude which tends to infinity as $\beta_{\rm ww} \to 1$ when the distribution becomes a delta function, the situation corresponding to a single-time-constant Debye system. The location of the maximum occurs at $\tau/\tau_{\rm ww} > 1$ for $\beta_{\rm ww} < 1$, and gradually decreases towards its limiting value of $\tau/\tau_{\rm ww} = 1$ when $\beta_{\rm ww} = 1$.[12] While originally an empirical model, there have been attempts to explain the success of this function using models for relaxation based on diffusion [201, 202]. Recently, Phillips [203] has reviewed 125 papers on the subject of stretched exponential relaxation published since 1977 and proposed a microscopic theory of the

[11]The stretched exponential relaxation was, in fact, first proposed some 150 years ago by Kohlrausch [199] who, while investigating the discharge of a Leyden jar, discovered that decay of the *residual* charge associated with the dielectric relaxation of the glass body of the jar displayed a stretched exponential behavior. Although it is not clear if Williams and Watts [176] had known about Kohlrausch's work when they published their paper, the distribution parameter $\beta_{\rm ww}$ is often called Kohlrausch-Williams-Watts relaxation constant.

[12]A detailed comparison of the Davidson-Cole and Williams-Watts functions has been presented by Lindsey and Patterson [200].

The Williams-Watts relaxation time distribution function is

$$G_{ww}(\tau, \beta_{ww}) := -\frac{\tau_{ww}}{\pi \cdot \tau} \cdot \sum_{n=0}^{n_{max}} \frac{(-1)^n}{n!} \cdot \sin(\pi \cdot \beta_{ww} \cdot n) \cdot \Gamma(\beta_{ww} \cdot n + 1) \cdot \left(\frac{\tau}{\tau_{ww}}\right)^{\beta_{ww} \cdot n + 1}$$

Below is a log-linear plot of $G_{ww}(\tau, \beta_{ww})$ over five decade of normalized quantity $\frac{\tau}{\tau_{ww}}$

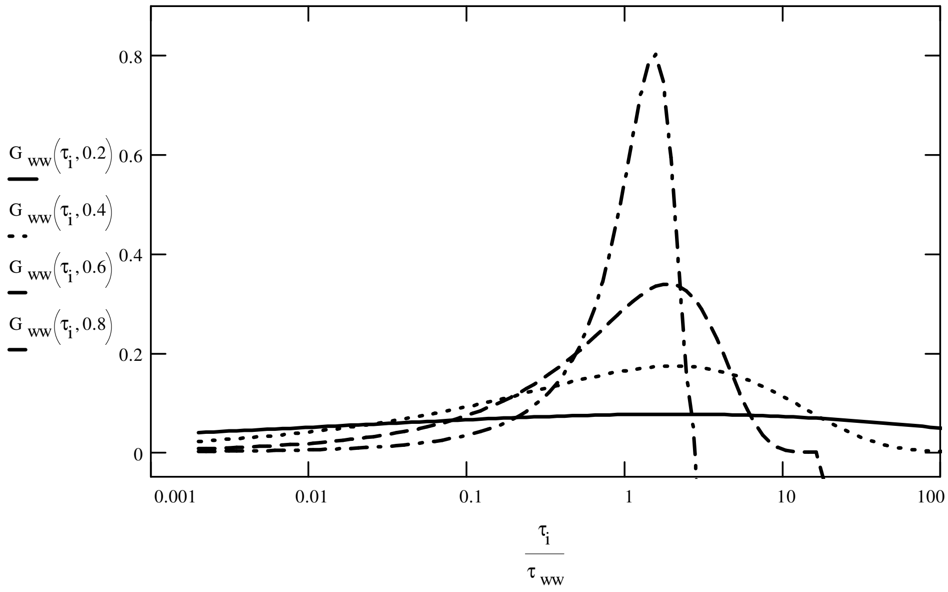

Figure 2-15: Mathcad worksheet calculating and displaying the Williams-Watts relaxation time distribution function for $\beta_{ww} = 0.2, 0.4, 0.6, 0.8$. The distribution function is very broad for the low values of β_{ww}, but tends asymptotically to a delta function at $\tau/\tau_{ww} = 1$ (Debye single-relaxation-time distribution) as $\beta_{ww} \to 1$.

In the following Cole-Cole plots, $k = \omega \cdot \tau_d$ is used as the parameter, ranging over ten decades:

$k_{min} := 0.00001 \quad k_{max} := 10000 \quad N := 300 \quad i := 1 .. N \quad k := \mathrm{LogRange}(k_{min}, k_{max}, N)$

In this notation, complex permittivities for the Debye, Cole-Cole, Davidson-Cole, and Williams-Watts models become:

$$\varepsilon_{DEBYE_i} := \varepsilon_{inf} + \frac{\varepsilon_0 - \varepsilon_{inf}}{1 + j \cdot k_i} \qquad \varepsilon_{CC_i} := \varepsilon_{inf} + \frac{\varepsilon_0 - \varepsilon_{inf}}{1 + (j \cdot k_i)^{\beta}} \qquad \varepsilon_{CD_i} := \varepsilon_{inf} + \frac{\varepsilon_0 - \varepsilon_{inf}}{(1 + j \cdot k_i)^{\beta}}$$

$$\varepsilon_{WW_i} := \varepsilon_{inf} + (\varepsilon_0 - \varepsilon_{inf}) \cdot \sum_{n=1}^{n_{max}} \frac{(-1)^{n-1}}{(k_i)^{n \cdot \beta}} \cdot \frac{\Gamma(n \cdot \beta + 1)}{\Gamma(n+1)} \cdot \left(\cos\left(\beta \cdot \frac{n \cdot \pi}{2}\right) - j \cdot \sin\left(\beta \cdot \frac{n \cdot \pi}{2}\right)\right)$$

First, we construct the Cole-Cole plots for each of the three models for $\beta := 0.7$

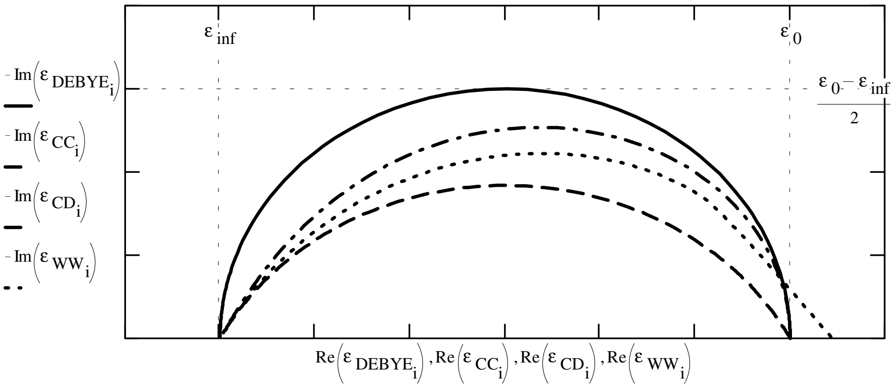

For comparison, the Cole-Cole plots for the same three models are shown below for $\beta := 0.4$

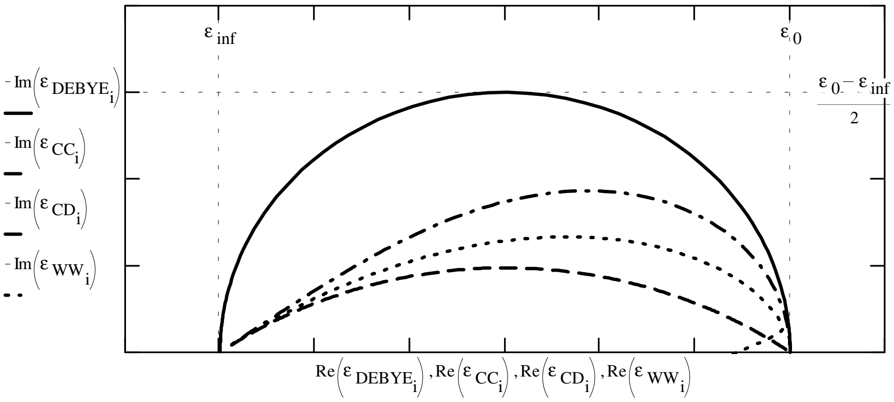

Figure 2-16: Mathcad worksheet calculating and displaying Cole-Cole plots of the Debye single relaxation time model (ε_{DEBYE}), Cole-Cole model (ε_{CC}), Davidson-Cole model (ε_{CD}), and Williams-Watts model (ε_{WW}).

The Williams-Watts relaxation time distribution function:

$$G_{ww}(\tau) := -\frac{\tau_{ww}}{\pi\cdot\tau}\cdot\sum_{n=0}^{n_{max}}\frac{(-1)^n}{n!}\cdot\sin\left(\pi\cdot\beta_{ww}\cdot n\right)\cdot\Gamma\left(\beta_{ww}\cdot n+1\right)\cdot\left(\frac{\tau}{\tau_{ww}}\right)^{\beta_{ww}\cdot n+1}$$

The Davidson-Cole distribution function:

$$G_{CD}(\tau) := \begin{cases}\dfrac{\sin\left(\pi\cdot\beta_{CD}\right)}{\pi}\cdot\left(\dfrac{\tau}{\tau_{CD}-\tau}\right)^{\beta_{CD}} & \text{if } \tau<\tau_{CD}\\ 0 & \text{otherwise}\end{cases}$$

The Cole-Cole distribution function:

$$G_{CC}(\tau) := \frac{1}{2\cdot\pi}\cdot\frac{\sin\left[\pi\cdot\left(1-\beta_{CC}\right)\right]}{\cosh\left(\beta_{CC}\cdot\ln\left(\dfrac{\tau}{\tau_{CC}}\right)\right)-\cos\left[\pi\cdot\left(1-\beta_{CC}\right)\right]}$$

Plotting the three functions on a log-linear plot vs normalized time constant:

$\beta_{ww} := 0.5$ $\beta_{CD} := 0.37$ $\beta_{CC} := 0.7$

$\tau_{ww} := 0.25$ $\tau_{CD} := 1.0$ $\tau_{CC} := 0.25$

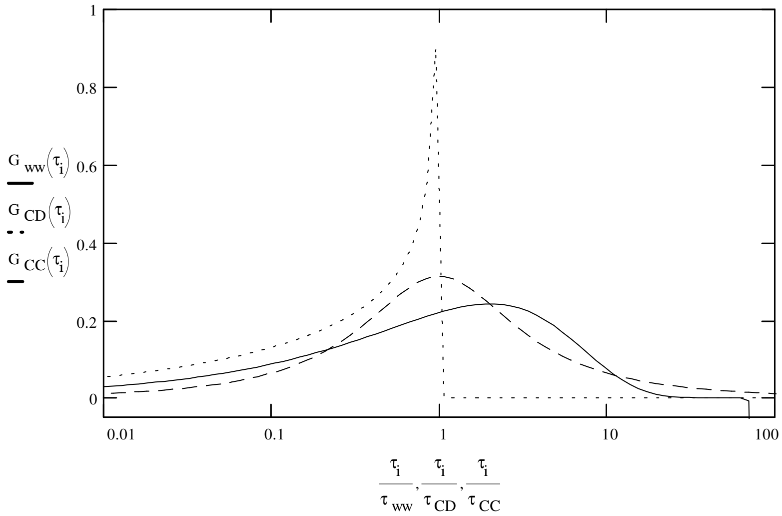

Figure 2-17: Mathcad worksheet calculating and displaying relaxation time distribution functions for Cole-Cole $G_{CC}(\tau/\tau_{CC})$, Davidson-Cole $G_{CD}(\tau/\tau_{CD})$, and Williams-Watts $G_{WW}(\tau/\tau_{WW})$ models. (The distribution function for the Debye single relaxation time model would appear as a delta function at $\tau/\tau_d = 1$ on the plot.) The constants (β's and τ's) for each models were chosen by a best fit of each function to a reliable set of experimental data [200].

Process	$\langle\tau\rangle$	$\langle\omega\rangle$
Debye	$\langle\tau\rangle_{\mathrm{D}} = \tau_d$	$\langle\omega\rangle_{\mathrm{D}} = \frac{1}{\tau_d}$
Cole-Cole	$\langle\tau\rangle_{\mathrm{CC}} = \tau_{\mathrm{CC}}$	$\langle\omega\rangle_{\mathrm{CC}} = \frac{1}{\tau_{\mathrm{CC}}}\tan\left(\frac{1}{\beta_{\mathrm{CC}}}\frac{\pi}{2}\right)$
Davidson-Cole†	$\langle\tau\rangle_{\mathrm{CD}} = \tau_{\mathrm{CD}}\beta_{\mathrm{CD}}$	$\langle\omega\rangle_{\mathrm{CD}} = \int_0^\infty \frac{G_{\mathrm{CD}}(\tau)}{\tau^2}d\tau$
Williams-Watts	$\langle\tau\rangle_{\mathrm{WW}} = \frac{\tau_{\mathrm{WW}}}{\beta_{\mathrm{WW}}}\Gamma\left(\frac{1}{\beta_{\mathrm{WW}}}\right)$	$\langle\omega\rangle_{\mathrm{WW}} \sim (d/dt)P_{\mathrm{WW}}(t)$ diverges‡

†The Davidson-Cole average relaxation frequency $\langle\tau\rangle_{\mathrm{CD}}$ can not be evaluated in closed form. To find it, a numerical integration of the relaxation times distribution function $G_{\mathrm{CD}}(\tau)$, as given by equation (2.53), must be performed.
‡As defined in Eqn. (2.55), $P_{\mathrm{WW}}(t) = e^{-(\frac{t}{\tau_{\mathrm{WW}}})^{\beta_{\mathrm{WW}}}}$.

Table 2.1: The average relaxation times $\langle\tau\rangle$ and the average relaxation frequencies $\langle\omega\rangle$ for various dielectric relaxation models considered in the text in terms of the parameters of those models.

Kohlrausch-Williams-Watts relaxation constant β_{ww} based on axiomatic set theory.

Deviations from the Debye behavior: A "many body interactions" approach

The dielectric relaxation models discussed thus far (Cole-Cole, Davidson-Cole, and Williams-Watts) have all taken the view that the nonexponential (non-Debye) relaxation behavior results from a superposition of exponentially relaxing processes with a particular distribution of relaxation times (Fig. 2-13). A completely different approach was taken by another group of researchers, lead by Jonscher [177, 204] who suggested that the relaxation behavior at the molecular level is intrinsically nonexponential, possibly resulting from cooperative molecular motions.

According to Jonscher [177, 205], the prevailing form of the frequency dependence of the dielectric loss peaks may be represented by the empirical law combining two power laws, respectively below and above the peak frequency ω_p

$$\varepsilon''(\omega) \sim \frac{1}{(\omega/\omega_p)^{-m} + (\omega/\omega_p)^{1-n}} \tag{2.58}$$

in which the exponents m and $1 - n$ fall in the range $(0, 1)$ and the peak frequency

ω_p is generally temperature dependent. The applicability of this empirical relation is limited at low frequencies by the onset of direct current conduction, while at the higher frequencies perturbing processes are often visible arising from the presence of some series resistance in the measuring system, or from the overlap of some other loss processes. Note that, while the relaxation models discussed previously all have only one parameter, the Jonscher model represented by Eqn. (2.58) is a two-parameter model.

To explain the two different and independent dielectric loss exponents to the left and to the right of the peak frequency ω_p (a feature characteristic of relaxation processes in many dielectric materials), Jonscher *et al.* developed the so-called *many-body universal model of dielectric relaxation* [205, 206], which was subsequently extended by the quantum-mechanical interpretation of Dissado and Hill [207, 208]. This model is based on a combination of single-particle and many-body transitions shown in the energy diagram of Fig. 2-18 which represents the potential energy of an assembly of a large number of interacting dipoles or charged particles in a two-level system. The large excitation energy Δ corresponds to the "large" transitions of single particles from an orientation or position corresponding to one of the two preferred states to the other allowed position or orientation. The bottoms of the potential wells are split by an energy $2B_{\text{eff}}$ which is determined by local conditions and by the externally applied field E. The shading of the bottoms of the potential wells represents the correlated states of width 2ζ shown in Fig. 2-18. The model recognizes three types of transitions denoted, respectively, by the arrows a, a', b, and c. Transitions a and a' correspond to the large single-particle transitions over the barrier height Δ, with thermal excitation in the case a and with partial tunneling in case a'. Transitions b and c, on the other hand, are configurational tunneling small transitions which do not involve thermal assistance.

The *small flip transitions* denoted by the arrow b in Fig. 2-18 represent a tunneling mode between different system configurations giving a net change of the total

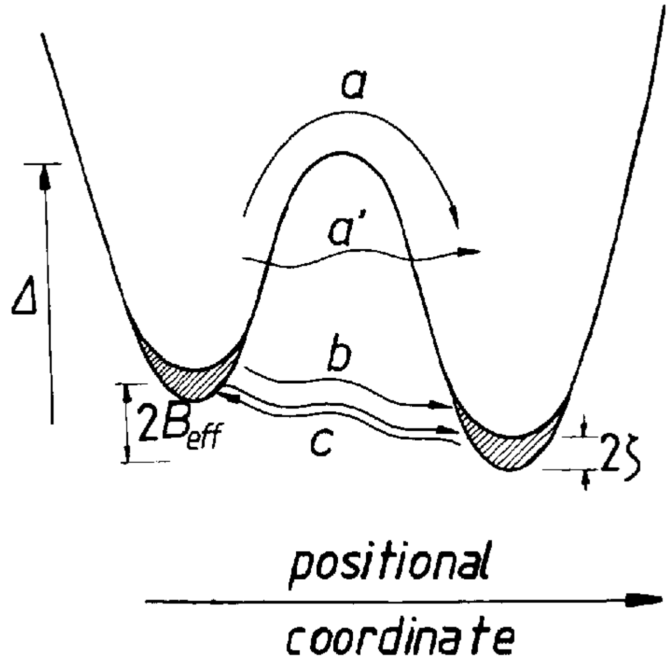

Figure 2-18: The potential energy diagram of a many-body two-level system representing the energy of a large number of interacting systems. The two wells correspond to the preferred orientations or positions. The splitting of the bottom by $2B_{\text{eff}}$ is shown; the shaded regions represent the energy states of width 2ζ resulting from particle interactions. Arrow a denotes large thermally assisted transitions over the barrier Δ, arrow a' is the same with tunnel assistance. Arrows b and c refer to configurational tunneling transitions of the *flip* and *flip-flop* types, respectively. (From Jonscher *et al.* [209].)

dipole moment. The *flip* transition constitutes the dominant polarization relaxation mechanism at high frequencies, $\zeta \ll \omega \ll \omega_p$, where $\zeta \simeq 10^{12}$ Hz is the phonon frequency of the system. These transition are thus the physical process behind the exponent n in Jonscher empirical "universal relaxation law" [Eqn. (2.58)]. On the other hand, the *flip-flop* processes denoted by the pair of arrows c in Fig. 2-18 represent the local fluctuations of the dipole moment which retain the average value of the total polarization. This mechanism, characterizing the response of the system at frequencies much lower than ω_p, is related to the exponent m in the empirical law of the dipolar response [Eqn. (2.58)].

The Dissado-Hill theory thus associates the exponent m in Eqn. (2.58) with the degree of correlation between the *flip-flop* transitions, and the exponent n with the degree of correlation of the *flip* transitions. In each case the value of unity corresponds to fully correlated transitions, and the value of zero — to uncorrelated transitions. The value $m = 0$ corresponds to completely uncorrelated *flip-flops*, giving the Davidson-Cole behavior [Eqn. (2.52).]

With increasing temperature, the correlation of the *flip* and *flip-flop* transitions is strengthened, increasing the values of the exponents m and n, as shown in Fig. 2-19. Note that the changes in the dielectric material itself (resulting, *e.g.*, from phase and structural transitions, diffusion of foreign species into the material, etc.) also alter the correlation of the *flip* and *flip-flop* transitions, and can thus affect the exponents m and n in a similar manner.

The sensitivity of the exponents m and n to the structure of the material represents one of the principal diagnostic uses of dielectric measurements. The shape of the loss spectrum represents a sensitive tool for the detection of order changes.

Summary

A summary of the various dielectric relaxation functions discussed in this section and their power-law exponents are displayed in Table 2.2.

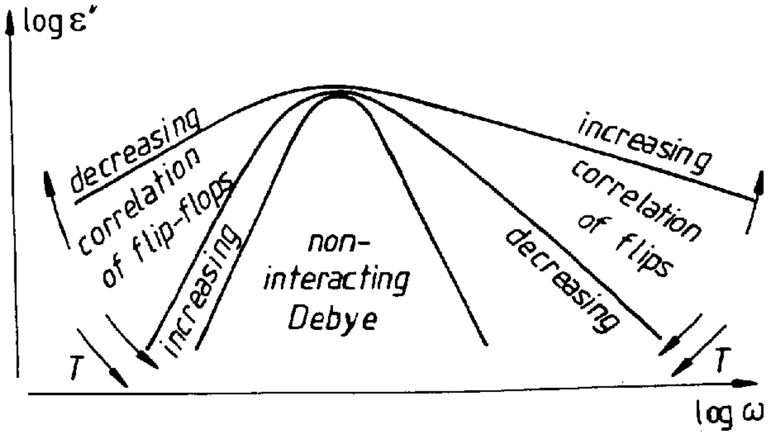

Figure 2-19: The effect of temperature on the shape of the loss peak of a dipolar material, as a consequence of changing correlations of *flip* and *flip-flop* transitions resulting from varying short-range order. The non-interacting Debye response is shown for comparison. (After Jonscher [210].)

Process	Normalized complex permittivity function	exponent for $\omega \ll \omega_p$		exponent for $\omega \gg \omega_p$	
		$\varepsilon'(\omega)$	$\varepsilon''(\omega)$	$\varepsilon'(\omega)$	$\varepsilon''(\omega)$
Debye (1929)	Eqn. (2.45)	2	1	-2	-1
Cole-Cole (1941)	Eqn. (2.50)	β_{cc}	β_{cc}	$-\beta_{cc}$	$-\beta_{cc}$
Davidson-Cole (1951)	Eqn. (2.52)	2	1	β_{cd}	β_{cd}
Williams-Watts (1970)	Eqn. (2.56)	2	1	$-\beta_{ww}$	$-\beta_{ww}$
Jonscher (1975)	Eqn. (2.58)	m	m	$n-1$	$n-1$

Table 2.2: A summary of various dielectric relaxation functions and their power-law exponents in the neighborhood of the peak frequency $\omega_p = \frac{2\pi}{\tau}$, where τ is the relaxation time parameter of the process in question.

2.3.4 Effect of Residual DC Conductivity

We saw from the Eqn. (2.44) on page 100 that the DC conductivity adds to the effective dielectric loss $\varepsilon''_{\text{eff}}(\omega)$ seen in a dielectric measurement:

$$\varepsilon_{\text{eff}}(\omega) = \varepsilon'(\omega) - j\left(\varepsilon''(\omega) + \frac{\sigma_0}{\omega\varepsilon_0}\right) \tag{2.59}$$

$$\varepsilon'_{\text{eff}}(\omega) = \varepsilon'(\omega) \tag{2.60}$$

$$\varepsilon''_{\text{eff}}(\omega) = \varepsilon''(\omega) + \frac{\sigma_0}{\omega\varepsilon_0}. \tag{2.61}$$

The frequency dependence of the loss factor described by Eqn. (2.59) is illustrated in Fig. 2-20. We see clearly that the DC conductivity σ_0 has a profound effect on the effective loss at low frequencies. Even a small σ_0 will dominate the dielectric response at sufficiently low frequencies because of the $1/\omega$ dependence. As σ_0 increases, it becomes increasingly difficult to discern the dipole loss peak. While it is still sometimes possible to extract the dipolar contribution to $\varepsilon''_{\text{eff}}$ even when σ_0 is large, an independent measurement of σ_0 is required.

Notation used in this worksheet: $\varepsilon_{inf} = \varepsilon_{\infty}$; $\varepsilon_0 = \varepsilon(0)$; $\omega = 2 \cdot \pi \cdot f$; ε_o=const; S $\equiv$ siemens

Effective permittivity $\varepsilon'(\omega)$ and loss $\varepsilon''(\omega, \sigma_0)$ are defined as follows:

$$\varepsilon'(f) := \varepsilon_{inf} + \frac{\varepsilon_0 - \varepsilon_{inf}}{1 + (2 \cdot \pi \cdot f \cdot \tau_d)^2} \qquad \varepsilon''(f, \sigma_0) := \frac{(\varepsilon_0 - \varepsilon_{inf}) \cdot 2 \cdot \pi \cdot f \cdot \tau_d}{1 + (2 \cdot \pi \cdot f \cdot \tau_d)^2} + \frac{\sigma_0}{2 \cdot \pi \cdot f \cdot \varepsilon_o}$$

Effective permittivity and loss are plotted below for τ_d=0.001sec and f=1Hz..30000Hz

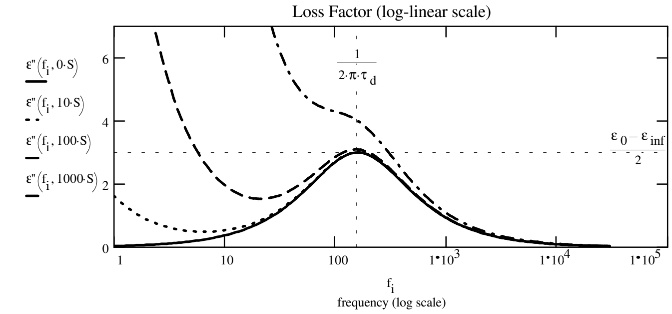

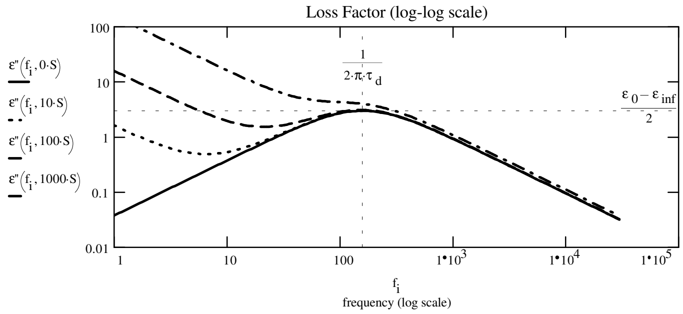

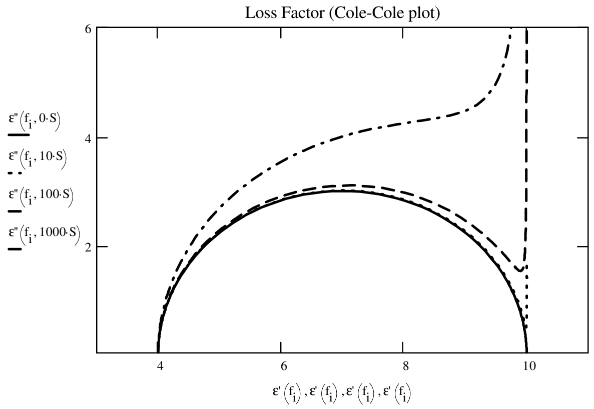

Figure 2-20: Mathcad worksheet illustrating the effective dielectric loss of a Debye dielectric having DC conductivity σ_0, for σ_0 equal to 0, 10, 100, and 1000 Siemens (solid, dotted, dashed, and dash-dotted traces, respectively). The frequency response of such a dielectric is shown here on the log-linear, log-log, and Cole-Cole plots. For each plot, the solid curves for which $\sigma_0 = 0$ S correspond to the ideal Debye dielectric similar to that of Figs. 2-12 and 2-14.